

Published in final edited form as:

Pain. 2011 October ; 152(10): 2323–2332. doi:10.1016/j.pain.2011.06.025.

Re-expression of the methylated *EDNRB* gene in oral squamous cell carcinoma attenuates cancer-induced pain

Chi T. Viet^{1,2}, Yi Ye¹, Dongmin Dang³, David K. Lam³, Stacy Achdjian³, Jianan Zhang¹, and Brian L. Schmidt^{1,4,*}

¹Department of Oral Maxillofacial Surgery, New York University, New York, NY, United States

²Oral and Craniofacial Graduate Program, University of California, San Francisco, San Francisco, CA, United States

³Department of Oral and Maxillofacial Surgery, University of California, San Francisco, San Francisco, CA, United States

⁴Bluestone Center for Clinic Research, New York University, NY, United States

Abstract

Endothelin-1 is a vasoactive peptide that activates both the endothelin A (ET_A) and endothelin B (ET_B) receptors, and is secreted in high concentrations in many different cancer environments. While ET_A receptor activation has an established nociceptive effect in cancer models, the role of ET_B receptors on cancer pain is controversial. *EDNRB*, the gene encoding the ET_B receptor, has been shown to be hypermethylated and transcriptionally silenced in many different cancers. In this study we demonstrate that *EDNRB* is heavily methylated in human oral SCC lesions, which are painful, but not methylated in human oral dysplasia lesions, which are typically not painful. ET_B mRNA expression is reduced in the human oral SCC lesions as a consequence of *EDNRB* hypermethylation. Using a mouse cancer pain model we show that ET_B receptor re-expression attenuates cancer-induced pain. These findings identify *EDNRB* methylation as a novel regulatory mechanism in cancer-induced pain and suggest that demethylation therapy targeted at the cancer microenvironment has the potential to thwart pain-producing mechanisms at the source, thus freeing patients of systemic analgesic toxicity.

Keywords

methylation; cancer pain; EDNRB; Endothelin B receptor; oral squamous cell carcinoma

INTRODUCTION

For almost all oral cancer patients, pain is rated as the worst symptom over all other symptoms. Oral cancer patients suffer severe pain for months and even years, preventing them from functioning normally [5; 6; 11; 12; 19]. The intensity of oral cancer pain is higher

© 2011 International Association for the Study of Pain. Published by Elsevier B.V. All rights reserved.

*Corresponding author: Brian L. Schmidt, DDS, MD, PhD, Bluestone Center for Clinical Research, New York University College of Dentistry, 421 First Avenue, 233W, New York, New York 10010, bls322@nyu.edu, Tel: 212-998-9543, Fax: 212-995-4843.

Conflict of Interest Statement: The authors have no conflict of interest to report.

Publisher's Disclaimer: This is a PDF file of an unedited manuscript that has been accepted for publication. As a service to our customers we are providing this early version of the manuscript. The manuscript will undergo copyediting, typesetting, and review of the resulting proof before it is published in its final citable form. Please note that during the production process errors may be discovered which could affect the content, and all legal disclaimers that apply to the journal pertain.

than that of other cancers [23; 24]. Oral cancer pain escalates with disease progression, so that terminal patients experience excruciating pain during their final months of life. Most oral cancer patients with severe pain are terminal patients. Approximately 50% of oral cancer patients will not be cured with surgery, chemotherapy or radiation therapy [36]. In the USA this group, which consists of approximately 40,000 new cases per year, is larger than those dying from melanoma, cervical cancer, or ovarian cancer [27].

Cancer pain, including oral cancer pain, is due to the production of nociceptive mediators, such as endothelin-1 (ET-1) into the cancer microenvironment [30; 35]. ET-1 is a vasoactive peptide that is produced and secreted into the cancer microenvironment in high concentration by many cancers including prostate, ovarian, breast, renal, bladder, cervical, bone and oral [2; 4; 13; 28; 30; 32–35; 37]. Oral squamous cell carcinoma (SCC), in particular, expresses extremely high levels of ET-1, compared to other cancers [29]. ET-1 binds two receptors, the endothelin A (ET_A) and the endothelin B (ET_B) receptors. ET_A receptors have an established role in neuropathic and inflammatory pain [1; 7; 14]. Activation of ET_A receptors also contributes to cancer pain. We have confirmed that it is the ET_A receptors on the primary afferent nerves within the cancer microenvironment that leads to significant pain [30; 32; 35].

Unlike ET_A receptor activation, evidence suggests that ET_B receptor activation has an anti-nociceptive effect in both non-cancer and cancer models [17; 28]. Khodorova and colleagues demonstrated that ET_B receptor activation on keratinocytes leads to an analgesic effect. Oral SCC consists of malignant keratinocytes. However, *EDNRB*, the gene encoding ET_B receptors, is frequently methylated in cancer. *EDNRB* methylation results in transcriptional silencing and has been demonstrated in cancers of many types, including lung, prostate, esophageal and nasopharyngeal cancer [15; 18; 21; 39].

In this study, we hypothesize that *EDNRB* is silenced through promoter methylation in oral SCC and that hypermethylation of this gene contributes to cancer induced pain. To investigate the role of *EDNRB* methylation in oral SCC pain we use a two-pronged approach. Firstly, to establish the clinical significance of *EDNRB* silencing on oral SCC pain, we quantify *EDNRB* promoter methylation in the biopsied tissues of oral dysplasia patients, and tumor and contralateral normal tissue from oral SCC patients. Secondly, we use a mouse oral cancer pain model to determine the behavioral effect of *EDNRB* re-expression *in vivo*.

MATERIALS AND METHODS

Tissue collection

All procedures were approved by the University of California, San Francisco Committee on Human Research. We enrolled oral SCC patients with the following inclusion criteria: 1) biopsy-proven oral SCC and 2) no history of prior surgical, chemotherapeutic, or radiation treatment for head and neck SCC. We collected tissue at time of surgery from the primary cancer site and contralateral normal epithelium as control. Samples were flash frozen in liquid nitrogen and stored in -80°C . Demographic and health information were recorded for each patient. Cancer patients were staged according to the American Joint Commission on Cancer tumor-node-metastasis (TNM) staging system [10]. Oral dysplasia tissue was obtained from paraffin-embedded tissues archived from excisional biopsies. Patient demographics and tumor characteristics are shown in Table 1.

RNA and DNA extraction

Thirty mg of each tissue collection sample was homogenized with a Mini Beadbeater-1 (BioSpec Products, Bartlesville, OK) and subject to RNA/DNA extraction with AllPrep

DNA/RNA Kit (Qiagen, Valencia, CA). RNA was eluted in a total volume of 50 μ l and DNA was eluted in a total volume of 100 μ l. RNA and DNA yield and quality were assessed with spectrometry (Nanodrop Technologies, Wilmington, DE).

Quantitative reverse transcription PCR (RT-PCR) analysis

RNA extracted from fresh frozen paired oral SCC and normal tissues from the 20 patients was converted to cDNA. mRNA was reverse transcribed with Random Hexamers. An 8 μ l cDNA aliquot was amplified in 25 μ l of 2x TaqMan universal master mix and 2.5 μ l of 20x Taqman primer and probe mix (Applied Biosystems, Carlsbad, CA) under the following PCR conditions: 2 minutes at 50°C, 10 minutes at 95°C, 50 cycles of 95°C for 15 seconds and 60°C for 1 minute. The Taqman gene expression assay used for *EDNRB* was Hs00240747_ml and does not detect residual genomic DNA. Human GUSB (product 4326320E) was used as the endogenous control (Applied Biosystems, Carlsbad, CA). Using *GUSB* as an internal locus control and the $2^{-\Delta\Delta C_t}$ quantitation method on Microsoft Excel, relative *EDNRB* transcript levels were obtained. Each sample was measured in duplicate.

Quantitative methylation analysis

Quantitative methylation analysis of the *EDNRB* promoter was performed through the Genome Analysis Core Facility at the University of California San Francisco, using the EpiTYPER assay (Sequenom, San Diego, CA) in conjunction with the MassARRAY system. The target region was located at chr13:78492226–78493582 on the antisense strand of the human genome on the UCSC Genome Browser. This target region includes a CpG island of 77 CpG sites and spans from –792 to +451 relative to the *EDNRB* transcription start site (GenBank entry AY275463.1). At least 1 μ g of DNA from each sample was treated with sodium bisulfite using the EZ DNA methylation kit (Zymo Research, Orange, CA) and the converted DNA was amplified by PCR. Primer sequences were designed with EpiDesigner software and are listed in Table 2. The PCR product was treated with shrimp alkaline phosphate and served as the template for transcription according to manufacturer's instructions. The samples were spotted on a 384-pad Spectro-CHIP and analyzed using a MassARRAY analyzer compact MALDI-TOF MS. Methylation calls were analyzed using EpiTyper software v1.0 to produce quantitative results for each CpG unit, which consists of a single CpG site or aggregate of adjacent CpG sites. Fully methylated DNA was used as positive control and water was used as negative control.

Recombinant adenovirus and *in vitro* transduction

A pCMV6-AC-GFP plasmid with GFP-tagged ORF clone of human *EDNRB*, transcript variant 1, was purchased from Origene (Rockville, MD). Subcloning of the plasmid and viral particle purification were completed through Viraquest (North Liberty, IA). Adenovirus containing only GFP was also obtained from Viraquest for use as a transduction control. The human head and neck cancer cell line derived from human tongue SCC, HSC-3 (ATCC, Manassas, VA), was transduced with recombinant adenovirus (Ad-EDRN or Ad-GFP) at increasing multiplicities of infection (MOI; number of viral particles per cell), at 50, 100, and 200. Transduction was performed in Dulbecco's Modified Eagle Medium (DMEM) with 4.5 g/L glucose, l-glutamine and sodium pyruvate, supplemented with 2% fetal bovine serum (FBS), 25 μ g/mL fungizone, 100 μ g/mL streptomycin sulfate, and 100 U/mL penicillin G. Twenty-four hours following transduction, cell media was changed to DMEM containing 10% FBS and the supplements mentioned above. mRNA quantification of transduced cells was performed using RT-PCR.

Immunofluorescence

Immunofluorescence was performed to evaluate the expression of the transgenes. HSC-3 cells were transduced with recombinant adenovirus at increasing multiplicities of infection. Twenty-four hours after transduction they were trypsinized and grown overnight at 37°C on 12-mm glass cover slips, stabilized in a 6-well plate with DMEM containing 10% fetal bovine serum and the aforementioned supplements. The cells were washed twice with PBS, fixed in ice-cold acetone for 5 minutes at room temperature (RT), permeabilized with 0.2% Triton X-100 for 15 minutes, washed three times in PBS then non-specifically blocked with 3% bovine serum albumin (BSA) for 2 hours. Incubation with primary rabbit polyclonal ET_B receptor antibody (Abeam Inc., Cambridge, MA) diluted 1:500 in 3% SA was performed at RT for 2 hours followed by incubation with goat anti-rabbit Texas Red-conjugated IgG secondary antibody (Jackson ImmunoResearch Laboratories, Inc., West Grove, PA) diluted 1:200 in 3% BSA for 1 hour at RT. Nuclei were stained with 1:500 Hoechst stain (Invitrogen, Carlsbad, CA). Cover slips were washed and mounted on slides in Gel/Mount mounting medium (Biomedica Crop., Foster City, CA) and visualized on the Zeiss AxioImager 2. Fluorescence quantification of captured images was performed with CellProfiler software. Data were manipulated according to the developer's instructions.

ELISA measurement of HSC-3 supernatant

ET-1 levels were quantified in the supernatant of nontransduced HSC-3 cells and Ad-EDNRB transduced HSC-3 cells. The samples were prepared as follows. Cells were grown to 60% confluency in 24-well plates and transduced in DMEM with 2% FBS. Twenty-four hours following transduction, transduction media was replaced with 1 ml DMEM containing 10% FBS and supplements. Control nontransduced HSC-3 cells were treated similarly. Cells were incubated for 4 hours at 37°C. Cell supernatant was collected and 10 µl Halt Protease Inhibitor (Thermo Scientific, Rockford, IL) added. Samples were added to the ET-1 ELISA plate (Assay Designs, Plymouth Meeting, PA) and ELISA was performed according to manufacturer's instructions. To perform the beta-endorphin ELISA, cells were incubated for 1 hour at 37°C. Cell supernatant was collected similarly and added to the beta-endorphin ELISA plate (MD Biosciences, St. Paul, MN). Samples were run in duplicate and measured using a spectrophotometer at recommended wavelengths.

Cancer pain mouse model

The cancer pain mouse model was produced as previously described [29]. Experiments were performed on 4 week-old adult female BALB/c, athymic, immunocompromised mice weighing 16–20 g at the time of human oral SCC inoculation. The mice were housed in a temperature-controlled room on a 12:12 h light cycle (0700–1900 h light), with unrestricted access to food and water. All the procedures were approved by the University of California, San Francisco Committee on Animal Research. Researchers were trained under the Animal Welfare Assurance Program. The mice were divided into three inoculation groups: (1) Ad-EDNRB transduced in HSC-3 (n=6), (2) Ad-GFP transduced in HSC-3 (n=6), or (3) HSC-3 (n=5). Inoculation of HSC-3 cells was performed 48 hours after adenovirus transduction, as preliminary characterization of the adenoviruses showed maximal ET_B receptor or GFP expression by 24 hours. Approximately 5×10^6 cells from each group were suspended in a mixture of 35 µl of Matrigel (Becton Dickinson & Co., Franklin Lakes, NJ) and 15 µL DMEM and inoculated into the plantar surface of the right hind paw under isoflurane inhalational anesthesia.

Paw withdrawal and paw volume measurement

Paw withdrawal testing was performed as described previously [29]. Testing was performed by an observer blinded to the experimental groups between 0900 and 1200 h. Mice were

placed in a plastic cage with a wire mesh floor which allowed access to the paws. Fifteen minutes were allowed for acclimation prior to testing. The probe was applied to the mid-plantar right hind paw. Paw withdrawal thresholds were determined in response to pressure from an electronic von Frey anesthesiometer (2390 series, IITC Life Sciences, Woodland Hills, CA). The amount of pressure (g) needed to produce a paw withdrawal response was measured six times on each paw separated by 3 min intervals to allow resolution of previous stimuli. The results of the six values were averaged for each paw for that day. Paw volume measurements were performed with a plethysmometer (IITC Life Sciences, Woodland Hills). The paw was inserted into a water cell of which pressure is changed due to the immersion. The pressure change was calibrated in milliliters and shown on an electronic monitor. The measurements were accurate by .001 ml. Triplicate measurements were taken for each mouse. Paw withdrawal and paw volume measurements were made at -2, 0, 4, 7, 9, 11, 13, 15, 18 and 21 days relative to inoculation of HSC-3 cells.

RESULTS

Oral dysplasia and SCC patient demographics

A total of 20 patients with biopsy-proven oral SCC were enrolled in the study. Patient demographics and tumor characteristics are described in Table 1. Nine men and eleven women were enrolled, with an age range of 49–93 and a median age 62. Pathology reports for all patients were reviewed to confirm the diagnosis of oral SCC. Tumor staging was also confirmed. None of the oral SCC patients had a cancer of another histologic type during the period of the study. A total of eight patients with biopsy-proven oral dysplasia were enrolled, with an age range of 50–89 and a median age of 69.5.

Higher EDNRB methylation in human oral SCC than normal tissue

A CpG island of 77 CpG sites in the *EDNRB* promoter was identified on UCSC Genome Browser. Primers were designed using EpiDesigner software. The primer sets are detailed in Table 2. Taken together, the four primer pairs span the region -792 to 451 relative to the *EDNRB* transcription start site (GenBank entry AY275463.1). The PCR products of the second and third primer sets overlapped each other by 188 bases. Due to the proximity of many CpG sites, not all CpG sites could be quantified. The four primer sets had the ability to quantify methylation at 61 out of the total 77 CpG sites, resulting in a total coverage of about 80%. The location of quantified sites is detailed in Figure 1.

Methylation was quantified using the MassARRAY System. The result was a methylation value for a CpG unit, which consisted of a single CpG site or aggregate of adjacent CpG sites. Methylation values ranged from 0 to 1, with 1 signifying 100% methylation of the CpG unit in the sample. Figure 1 shows heat maps of methylation values obtained for the CpG units within each *EDNRB* PCR product. Normal tissue has relatively low baseline methylation. Comparing the different *EDNRB* PCR products, EDNRB 4 has a higher baseline methylation level in normal tissues than any of the other products. EDNRB 4 is also the only product to be entirely located downstream of the transcription start site, in exon 1.

Comparing the paired oral SCC to normal tissue, oral SCC tissue clearly has higher methylation than contralateral-matched normal tissue in all patients, at almost all CpG units. Out of the 61 CpG sites quantified, the average increase in methylation in oral SCC tissue compared to the corresponding normal tissue was at least 10% (methylation value change 0.1) in 57 sites (93% of sites). The four sites with a methylation value change of lower than 0.1 were CpG 1, 2, 3, and 6 in PCR product EDNRB 4, which starts 151 downstream of the transcription start site. Table 3 summarizes the mean methylation difference between oral SCC and normal tissue at each CpG unit, and the corresponding p-value from the Student's

t-test. Figure 2a shows box plots representing methylation difference values between oral SCC and normal tissue, for each of the four *EDNRB* PCR products. The difference values were averaged across all patients for each CpG site. The median, 10th, 25th, 75th and 90th percentiles were calculated for each group of CpG sites within a PCR product. PCR product EDNRB 2 had the highest methylation increase from normal to oral SCC tissue, with a median increase of .34 (34%). PCR products EDNRB 1 and 3 had a median increase in methylation of 0.25 (25%). Due to already higher baseline methylation levels of EDNRB 4 in normal tissues, the median increase of methylation in oral SCC tissue was 0.13 (13%). The Mann Whitney Rank Sum Test demonstrated that there was a significant difference between methylation values of oral SCC tissue and the matched normal tissue. Methylation values for each sample were averaged across all CpG sites within each PCR product and oral SCC tissue was compared to normal tissue. There was a significant difference ($p < .001$) in methylation between cancer and normal tissue in all four PCR products, indicating significant increase in methylation spanning the whole *EDNRB* promoter in oral SCC.

These results show that there are consistently higher methylation levels in oral SCC tissue in 93% of the queried CpG sites in 100% of sample pairs. Furthermore, there is a larger increase in methylation in the first three PCR products, EDNRB 1, 2 and 3, which are located upstream of the transcription start site. There is a modest increase in methylation of CpG sites of EDNRB 4, which is located downstream of the transcription start site. These results suggest that increase in methylation upstream, and not downstream, of the *EDNRB* transcription start site, has a more significant contribution to carcinogenesis.

Oral SCC patients demonstrate higher *EDNRB* methylation than oral dysplasia patients

Methylation quantification of *EDNRB* was performed on paraffin-embedded tissue of eight biopsy-proven oral dysplasia patients. Methylation results were then averaged and compared to the average methylation of oral SCC tissue. EDNRB 2 PCR product was too long and could not be reliably amplified using DNA purified from the paraffin embedded tissue of dysplasia patients. Oral SCC tissue demonstrated higher methylation than oral dysplasia tissues at all queried CpG sites, and were on average 20% higher (range of 6–39%) (Figure 3). There was a significant difference between the methylation values at almost all CpG sites (Mann Whitney Rank Sum Test).

***EDNRB* promoter methylation levels are higher in patients with nodal metastasis**

We also classified our patients by their N staging in their TNM classification and compared *EDNRB* methylation among the different N stages. There were eleven patients with N staging of 0, three patients with N staging of 1, and six patients with N staging of 2. Figure 4 is a line and scatter plot graphing the difference in methylation between the oral SCC tissue of a patient and the normal tissue. The patients are categorized into the three possible N staging groups; each point on the graph represents the average of difference in methylation of oral SCC versus normal tissue, of all samples in the group. The plot shows average methylation difference in CpG sites comprised in PCR product EDNRB 1. These sites are the extreme 5' end of the CpG island in the *EDNRB* promoter, and are located -792 to -425 upstream of the transcription start site. The plot shows that methylation difference is lowest in the N=0 group, and is highest in the N=2 group. There was a significant difference between the three groups in seven of the ten CpG units, equating to 11 or 16 CpG sites (ANOVA). Furthermore, the N=2 group as significantly different from the N=0 group in all seven CpG units, and the N=1 as significantly different from the N=0 group at one CpG unit ($p < .05$, Holm-Sidak).

EDNRB mRNA expression is lower in oral SCC than normal tissue

The fold-change in expression of *EDNRB* in normal tissue compared to oral SCC tissue in the same patient was calculated. A fold change of more than 1 indicated that *EDNRB* expression was higher in the normal tissue than in the oral SCC tissue. Of the 20 patients, the average fold change of *EDNRB* expression was 10.9. Nineteen out of 20 patients (95%) had higher *EDNRB* expression in normal tissue than oral SCC tissue (range in fold change of 1.15–53.0), indicating downregulation of *EDNRB* in the oral SCC state. Figure 2b compares *EDNRB* expression in oral SCC to normal tissue. *EDNRB* expression in normal tissue is significantly higher than oral SCC tissue ($p < 0.001$, Student's t-test).

Oral SCC cells transduced with Ad-EDNRB express high levels of EDNRB mRNA and ET_B receptor

The *EDNRB* promoter in human oral cancer tissue is heavily methylated, whereas the *EDNRB* promoter in normal and dysplastic oral tissues has low levels of methylation. Furthermore, EDNRB mRNA expression was considerably reduced in cancer tissue compared to normal tissues. We wanted to explore the biological role of silenced EDNRB expression in the cancer microenvironment. To do so, we used adenoviruses to overexpress *EDNRB in vitro*. To overexpress *EDNRB* we transduced oral SCC cells (HSC-3) with adenovirus containing the *EDNRB* gene. HSC-3 has nondetectable levels of EDNRB mRNA and, when methylation levels of the *EDNRB* promoter in this cell line were quantified using MassARRAY, an average methylation level for all CpG sites was 85%. Our goal was to re-express *EDNRB* and determine the effect on the cancer microenvironment *in vitro*.

To confirm overexpression subsequent to transduction, immunofluorescence with EDNRB antibody was performed. ET_B receptor expression in oral SCC cells was minimal, while transduction of Ad-EDNRB resulted in a marked increase in ET_B receptor membrane expression. Figure 5 shows images from cells transduced at 200 MOI, as 50 MOI and 100 MOI show similar trends.

RT-PCR was performed on mRNA extracted from nontransduced oral SCC cells and oral SCC cells transduced with Ad-EDNRB at increasing MOI. RT-PCR results shown in figure 6a illustrate a dose-dependent increase in EDNRB mRNA expression with increasing MOI. Oral SCC cells transduced with Ad-EDNRB at 200 MOI express 3×10^7 more mRNA than nontransduced oral SCC.

Figure 6b illustrates relative ET_B receptor expression in the three groups of oral SCC cells: nontransduced, Ad-GFP and Ad-EDNRB transduced at 200 MOI. ET_B receptor expression was quantified relative to nontransduced oral SCC cells, which have a relative expression of 1. While Ad-GFP transduced cells do not exhibit a difference in ET_B receptor expression, those transduced with Ad-EDNRB express 9.6 times more ET_B receptor than control oral SCC cells.

Oral SCC cells transduced with Ad-EDNRB secrete lower levels of ET-1 and higher levels of beta-endorphin

We have previously shown that oral SCC cells secrete very high levels of ET-1 [29]. We wanted to determine the effect of re-expressing ET_B receptor on ET-1 levels in oral SCC cells. We transduced oral SCC cells with Ad-EDNRB and then performed ELISA to measure ET-1 in the supernatant. Our results showed that oral SCC cells transduced with Ad-EDNRB secreted lower levels of ET-1 than nontransduced oral SCC. Supernatant of oral SCC cells transduced with Ad-EDNRB at 200 MOI had an average ET-1 concentration of

9.2 pg/l. Supernatant of control oral SCC cells, which were transduced with Ad-GFP, had an average ET-1 concentration of 37.3 pg/l.

Conversely, oral SCC cells transduced with Ad-EDNRB secreted more beta-endorphin than control. Supernatant beta-endorphin concentration of Ad-EDNRB-transduced oral SCC cells was 0.94 ng/ml. Control cells, which were transduced with Ad-GFP, secreted an average of 0.66 ng/ml. Each sample was run in duplicate, so statistical significance was not assessed.

Transduction of Ad-EDNRB decreases nociception without affecting tumor size in a cancer mouse model

Human cancer cell proliferation and cancer-induced mechanical allodynia were assessed in the three orthotopic mouse model groups: (1) Ad-EDNRB-transduced HSC-3 tumors; (2) Ad-GFP-transduced HSC-3 tumors; and (3) non-transduced HSC-3 tumors. The results up to 21 days after inoculation of HSC-3 tumors showed that the three groups had similar paw volume, indicating that overexpressing *EDNRB* did not significantly alter tumor proliferation (Figure 7a). Overexpression of *EDNRB* did, however, affect cancer-induced mechanical allodynia. Cancers expressing *EDNRB* displayed a significantly higher paw withdrawal threshold than either the nontransduced cancer or the cancer expressing GFP. Figure 7b shows that mice with cancers expressing *EDNRB* have paw withdrawal thresholds that stabilized at 48% below baseline, regardless of the fact that tumor size was increasing. The average paw withdrawal threshold of these mice on day 21 was 2.12 g, approximately 48% of the day 0 threshold of 4.09 g. The Ad-GFP transduced HSC-3 cancers and non-transduced HSC-3 cancer groups showed a 65% (day 0 average = 4.06g; day 21 average = 1.41 g) and 67% (day 0 average = 3.90g; day 21 average = 1.29g) reduction in paw withdrawal threshold, respectively. The baseline paw withdrawal of the three groups was not significantly different from each other. The paw withdrawal threshold of tumors overexpressing *EDNRB* was significantly higher than the control groups, indicating lower mechanical allodynia (Student's t test, p-values as indicated in Figure 7b).

DISCUSSION

In this study we demonstrate that methylation of *EDNRB* is a novel mechanism generating cancer pain and expression of the ET_B receptor reverses cancer pain. Evidence supporting this result includes our finding that *EDNRB* is heavily methylated in painful human oral cancer specimens compared to matched normal controls and oral dysplasia, which is typically not painful. In addition, oral cancer specimens express less *EDNRB* mRNA than matched normal controls, indicating a correlation between increased *EDNRB* methylation and decreased mRNA expression. Using a cancer pain mouse model we show that re-expression of ET_B receptors using adenoviruses leads to significant attenuation of cancer pain behavior. This study is the first to demonstrate that gene methylation could be a significant mechanism causing cancer-induced pain, and that reversing the gene silencing process with targeted therapy could produce analgesia.

Oral cancer is notoriously painful. The pain is consistent with mechanical allodynia and severely limits function [6; 19]. We used resected cancer specimens and anatomically matched normal oral tissue from the same patients to evaluate *EDNRB* methylation. This approach allows for an accurate analysis of methylation levels associated with carcinogenesis. We quantified methylation in the promoter region of *EDNRB* spanning 77 CpG sites and 1.2 kilobases, which to date represents the most comprehensive methylation panel of *EDNRB* in normal, dysplastic, and cancer tissue. Oral cancer patients demonstrated higher methylation of *EDNRB* than oral dysplasia patients at all queried CpG sites. In our recent study we quantified pain in our cohort of oral dysplasia and oral cancer patients using the validated UCSF Oral Cancer Pain Questionnaire [20]. We demonstrated that only oral

cancer patients, and not dysplasia patients, reported significant levels of spontaneous and function-related pain, with function-related pain being markedly pronounced. Additionally, when we compared methylation frequency in patients with and without nodal metastasis, patients with an N staging of 2 showed significantly higher methylation than patients with an N staging of 0 in the 5' end of the *EDNRB* promoter. These results correlate with our previous finding that oral cancers that are metastatic are more painful [6].

Next, we wanted to understand the biologic significance of *EDNRB* expression on cancer-induced pain. Cancer pain has been hypothesized to result from either a tumor-mass effect or the activation of primary afferent nociceptors by mediators liberated by the cancer [3; 8; 9; 22; 25]. The tumor-mass effect is unlikely because even small carcinomas are painful [6]. We hypothesized that cancer pain results from an imbalance in pain-producing and pain-relieving mediators within the cancer microenvironment. The endothelin axis provides a compelling example of this imbalance. We have previously shown that for the human oral SCC cell line, the mRNA for ET-1 is nearly doubled, while mRNA for ET_B receptors is down-regulated compared to normal oral keratinocytes [33]. Similarly in lung cancer, ET_B receptors are down-regulated via promoter methylation [18]. The ET_B receptors could mediate analgesia, attenuating the acute pain generated by ET-1 [16; 31]. This counterbalancing, pain-relieving effect could be lost in cancers because ET_B receptors are not expressed. We therefore proposed that if the promoter for ET_B receptors could be re-expressed then the receptor could be activated by ET-1. To test this hypothesis we developed a cancer mouse model in which ET_B receptors were re-expressed. Since there is currently no reliable method to demethylate a specific gene and activate its transcription, adenovirus transduction was the most feasible method of re-expression. Our results showed that mice with oral SCC tumors expressing *EDNRB* had significantly lower levels of mechanical allodynia than mice with oral SCC tumors that did not express *EDNRB*.

ET_B receptor expression leads to antinociception through two likely mechanisms: 1) activation of ET_B receptor, which activates an endogenous analgesic mechanism, and 2) reduced ET-1 secretion by the carcinoma. The endogenous analgesic mechanism by ET_B receptor activation was first demonstrated by Khodorova et al., who also showed that the analgesic cascade involved release of beta-endorphin [17]. We demonstrated in this study that re-expression of ET_B receptor resulted in increased secretion of beta-endorphin into the oral SCC supernatant. These results correspond to our earlier results where treatment of oral SCC cells with an ET_B receptor agonist caused increased secretion of beta-endorphin compared to control cells [33]. Support for the second analgesic mechanism comes from our finding that ET-1 levels in the cell supernatant were significantly lower in oral SCC re-expressing the ET_B receptor. ET_B receptors have a known role in ET-1 clearance and inhibiting ET-1 secretion in keratinocytes [26; 38]. Our previous studies in a mouse oral SCC model have shown that ET-1 protein and mRNA concentrations are markedly elevated in oral SCC tumors. These elevated ET-1 levels caused increased pain by activation of the ET_A receptor. Not only is ET-1 elevated in numerous cancer types, our studies on salivary biomarkers have shown that ET-1 is significantly elevated in saliva of patients with oral SCC compared to normal subjects [30]. High ET-1 concentration activates ET_A and downstream networks resulting in nociception. We also demonstrated that melanoma tumors of equal size to SCC tumors produced significantly less pain, since they had a lower ET-1 concentration. Therefore, cancer pain intensity depends more on ET-1 concentration in that tumor than tumor size itself [29]. From these cumulative findings we propose that increased concentration of ET-1 activates ET_A and subsequent nociceptive pathways, and re-expression of the ET_B receptor produces an analgesic effect by counter-regulating ET-1/ET_A nociceptive mechanisms.

For most cancer patients, uncontrollable pain creates a poor quality of life [5; 6; 11; 12]. Because improved chemotherapy and radiotherapy prolong survival, chronic cancer pain is a major public health problem. To date there is no effective treatment for chronic cancer pain. The role of gene methylation in cancer pain has not been previously demonstrated. The findings from this study establish gene methylation as a novel regulatory mechanism of cancer-induced pain. Furthermore, the findings suggest that targeted gene demethylation could serve as a novel analgesic therapy to chronic cancer pain. Such therapy targeted to the cancer microenvironment like we had demonstrated in this study could antagonize pain while minimizing systemic drug toxicity and solve the current public health problem of chronic cancer pain refractory to traditional therapeutics.

Acknowledgments

This work was supported by National Institutes of Health grant R21 DE018561.

References

1. Baamonde A, Lastra A, Villazon M, Bordallo J, Hidalgo A, Menendez L. Involvement of endogenous endothelins in thermal and mechanical inflammatory hyperalgesia in mice. *Naunyn Schmiedebergs Arch Pharmacol.* 2004; 369(2):245–251. [PubMed: 14661069]
2. Bagnato A, Tecce R, Di Castro V, Catt KJ. Activation of mitogenic signaling by endothelin 1 in ovarian carcinoma cells. *Cancer Res.* 1997; 57(7):1306–1311. [PubMed: 9102218]
3. Bjordal K, Kaasa S. Psychological distress in head and neck cancer patients 7–11 years after curative treatment. *Br J Cancer.* 1995; 71 (3):592–597. [PubMed: 7880743]
4. Carducci MA, Jimeno A. Targeting bone metastasis in prostate cancer with endothelin receptor antagonists. *Clin Cancer Res.* 2006; 12(20 Pt 2):6296s–6300s. [PubMed: 17062717]
5. Chaplin JM, Morton RP. A prospective, longitudinal study of pain in head and neck cancer patients. *Head Neck.* 1999; 21 (6):531–537. [PubMed: 10449669]
6. Connelly ST, Schmidt L. Evaluation of pain in patients with oral squamous cell carcinoma. *J Pain.* 2004; 5(9):505–510. [PubMed: 15556829]
7. Davar G, Hans G, Fareed MU, Sinnott C, Strichartz G. Behavioral signs of acute pain produced by application of endothelin-1 to rat sciatic nerve. *Neuroreport.* 1998; 9(10):2279–2283. [PubMed: 9694215]
8. Diener KM. Bisphosphonates for controlling pain from metastatic bone disease. *Am J Health Syst Pharm.* 1996; 53(16):1917–1927. [PubMed: 8862204]
9. Fujita T, Matsui M, Takaku K, Uetake H, Ichikawa W, Taketo MM, Sugihara K. Size- and invasion-dependent increase in cyclooxygenase 2 levels in human colorectal carcinomas. *Cancer Res.* 1998; 58(21):4823–4826. [PubMed: 9809985]
10. Greene, FL. American Cancer Society. American Joint Committee on Cancer. |. Title |, Vol. Volume |. City |: Publisher |, Year |
11. Hammerlid E, Bjordal K, Ahlner-Elmqvist M, Boysen M, Evensen JF, Biorklund A, Jannert M, Kaasa S, Sullivan M, Westin T. A prospective study of quality of life in head and neck cancer patients. Part I: at diagnosis. *Laryngoscope.* 2001; 111 (4 Pt 1):669–680. [PubMed: 11359139]
12. Hodder SC, Edwards MJ, Brickley MR, Shepherd JP. Multiattribute utility assessment of outcomes of treatment for head and neck cancer. *Br J Cancer.* 1997; 75(6):898–902. [PubMed: 9062413]
13. Honore P, Luger NM, Sabino MA, Schwei MJ, Rogers SD, Mach D, O'Keefe PF, Ramnaraine ML, Clohisy DR, Mantyh PW. Osteoprotegerin blocks bone cancer-induced skeletal destruction, skeletal pain and pain-related neurochemical reorganization of the spinal cord. *Nat Med.* 2000; 6(5):521–528. [PubMed: 10802707]
14. Jarvis MF, Wessale JL, Zhu CZ, Lynch JJ, Dayton BD, Calzadilla SV, Padley RJ, Opgenorth TJ, Kowaluk EA. ABT-627, an endothelin ET(A) receptor-selective antagonist, attenuates tactile allodynia in a diabetic rat model of neuropathic pain. *Eur J Pharmacol.* 2000; 388(1):29–35. [PubMed: 10657544]

15. Jeronimo C, Henrique R, Campos PF, Oliveira J, Caballero OL, Lopes C, Sidransky D. Endothelin B receptor gene hypermethylation in prostate adenocarcinoma. *J Clin Pathol.* 2003; 56(1):52–55. [PubMed: 12499435]
16. Khodorova A, Fareed MU, Gokin A, Strichartz GR, Davar G. Local injection of a selective endothelin-B receptor agonist inhibits endothelin-1-induced pain-like behavior and excitation of nociceptors in a naloxone-sensitive manner. *J Neurosci.* 2002; 22(17):7788–7796. [PubMed: 12196602]
17. Khodorova A, Navarro B, Jouaville LS, Murphy JE, Rice FL, Mazurkiewicz JE, Long-Woodward D, Stoffel M, Strichartz GR, Yukhananov R, Davar G. Endothelin-B receptor activation triggers an endogenous analgesic cascade at sites of peripheral injury. *Nat Med.* 2003; 9(8):1055–1061. [PubMed: 12847519]
18. Knight LJ, Burrage J, Bujac SR, Haggerty C, Graham A, Gibson NJ, Ellison G, Growcott JW, Brooks AN, Hughes AM, Xinarianos G, Nikolaidis G, Field JK, Liloglou T. Epigenetic silencing of the endothelin-B receptor gene in non-small cell lung cancer. *Int J Oncol.* 2009; 34(2):465–471. [PubMed: 19148482]
19. Kolokythas A, Connelly ST, Schmidt BL. Validation of the university of California san francisco oral cancer pain questionnaire. *J Pain.* 2007; 8(12):950–953. [PubMed: 17686656]
20. Lam D, Schmidt BL. Orofacial pain onset predicts transition to head and neck cancer. *Pain.* 2011 in press.
21. Lo KW, Tsang YS, Kwong J, To KF, Teo PM, Huang DP. Promoter hypermethylation of the EDNRB gene in nasopharyngeal carcinoma. *Int J Cancer.* 2002; 98(5):651–655. [PubMed: 11920632]
22. Mantyh PW, Clohisy DR, Koltzenburg M, Hunt SP. Molecular mechanisms of cancer pain. *Nature Rev Cancer.* 2002; 2(3):201–209. [PubMed: 11990856]
23. Mercadante S. Malignant bone pain: pathophysiology and treatment. *Pain.* 1997; 69(1–2):1–18. [PubMed: 9060007]
24. Mercadante S, Dardanoni G, Salvaggio L, Armata MG, Agnello A. Monitoring of opioid therapy in advanced cancer pain patients. *J Pain Symptom Manage.* 1997; 13(4):204–212. [PubMed: 9136231]
25. Morton RP. Life-satisfaction in patients with head and neck cancer. *Clin Otolaryngol.* 1995; 20(6):499–503. [PubMed: 8665706]
26. Nelson JB, Carducci MA. The role of endothelin-1 and endothelin receptor antagonists in prostate cancer. *BJU Int.* 2000; 85 (Suppl 2):45–48. [PubMed: 10781185]
27. Parkin DM, Pisani P, Ferlay J. Global cancer statistics. *CA Cancer J Clin.* 1999; 49(1):33–64. 31. [PubMed: 10200776]
28. Peters CM, Lindsay TH, Pomonis JD, Luger NM, Ghilardi JR, Sevcik MA, Mantyh PW. Endothelin and the tumorigenic component of bone cancer pain. *Neuroscience.* 2004; 126(4):1043–1052. [PubMed: 15207337]
29. Pickering V, Jay Gupta R, Quang P, Jordan RC, Schmidt BL. Effect of peripheral endothelin-1 concentration on carcinoma-induced pain in mice. *Eur J Pain.* 2008; 12(3):293–300. [PubMed: 17664075]
30. Pickering V, Jordan RC, Schmidt BL. Elevated salivary endothelin levels in oral cancer patients--a pilot study. *Oral Oncol.* 2007; 43(1):37–41. [PubMed: 16757207]
31. Piovezan AP, D'Orleans-Juste P, Souza GE, Rae GA. Endothelin-1-induced ET(A) receptor-mediated nociception, hyperalgesia and oedema in the mouse hind-paw: modulation by simultaneous ET(B) receptor activation. *Br J Pharmacol.* 2000; 129(5):961–968. [PubMed: 10696096]
32. Quang PN, Schmidt BL. Endothelin-A receptor antagonism attenuates carcinoma-induced pain through opioids in mice. *J Pain.* 2010; 11(7):663–671. [PubMed: 20071245]
33. Quang PN, Schmidt BL. Peripheral endothelin B receptor agonist-induced antinociception involves endogenous opioids in mice. *Pain.* 2010; 149(2):254–262. [PubMed: 20206445]
34. Rosano L, Salani D, Di Castro V, Spinella F, Natali PG, Bagnato A. Endothelin-1 promotes proteolytic activity of ovarian carcinoma. *Clin Sci (Lond).* 2002; 103 (Suppl 48):306S–309S. [PubMed: 12193110]

35. Schmidt BL, Pickering V, Liu S, Quang P, Dolan J, Connelly ST, Jordan RC. Peripheral endothelin A receptor antagonism attenuates carcinoma-induced pain. *Eur J Pain*. 2007; 11(4):406–414. [PubMed: 16807013]
36. Silverman, SJ. *Epidemiology*. D.C: Decker Inc; 1998.
37. Wacnik PW, Eikmeier LJ, Ruggles TR, Ramnaraine ML, Walcheck BK, Beitz AJ, Wilcox GL. Functional interactions between tumor and peripheral nerve: morphology, algogen identification, and behavioral characterization of a new murine model of cancer pain. *J Neurosci*. 2001; 21 (23): 9355–9366. [PubMed: 11717369]
38. Yohn JJ, Smith C, Stevens T, Morelli JG, Shurnas LR, Walchak SJ, Hoffman TA, Kelley KK, Escobedo-Morse A, Yanagisawa M, et al. Autoregulation of endothelin-1 secretion by cultured human keratinocytes via the endothelin B receptor. *Biochim Biophys Acta*. 1994; 1224(3):454–458. [PubMed: 7803503]
39. Zhao BJ, Sun DG, Zhang M, Tan SN, Ma X. Identification of aberrant promoter methylation of EDNRB gene in esophageal squamous cell carcinoma. *Dis Esophagus*. 2009; 22(1):55–61. [PubMed: 18564167]

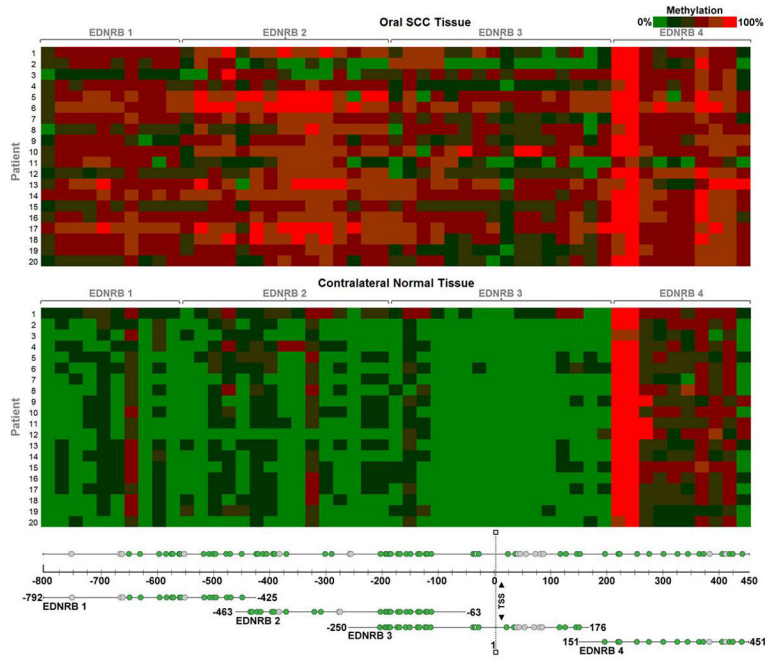


Figure 1. Heat map of *EDNRB* methylation

The heat map signifies quantified methylation values. Within each cell is the methylation value of a patient sample at a particular CpG unit. The values are color coded using a green-red scale, where green is low methylation and red is high methylation. The top heat map shows methylation values of oral SCC tissue. The bottom heat map shows methylation values of contralateral normal tissue. The *EDNRB* PCR product in which the CpG unit is located is indicated in the gene map. Each PCR product is shown in relation to the *EDNRB* promoter region and exon 1. Start and end bases for each product are noted; bases are numbered relative to the transcription start site (TSS). PCR product EDNRB 1 surveys the extreme 5' end of the CpG island. EDNRB 2 and 3 are located proximal to the TSS. They overlap each other by 188 bases. EDNRB 4 is located in exon 1 of the gene. Green circles denote the 61 out of 77 CpG sites whose methylation frequencies were quantified. Grey circles denote the 16 CpG sites that were not quantified.

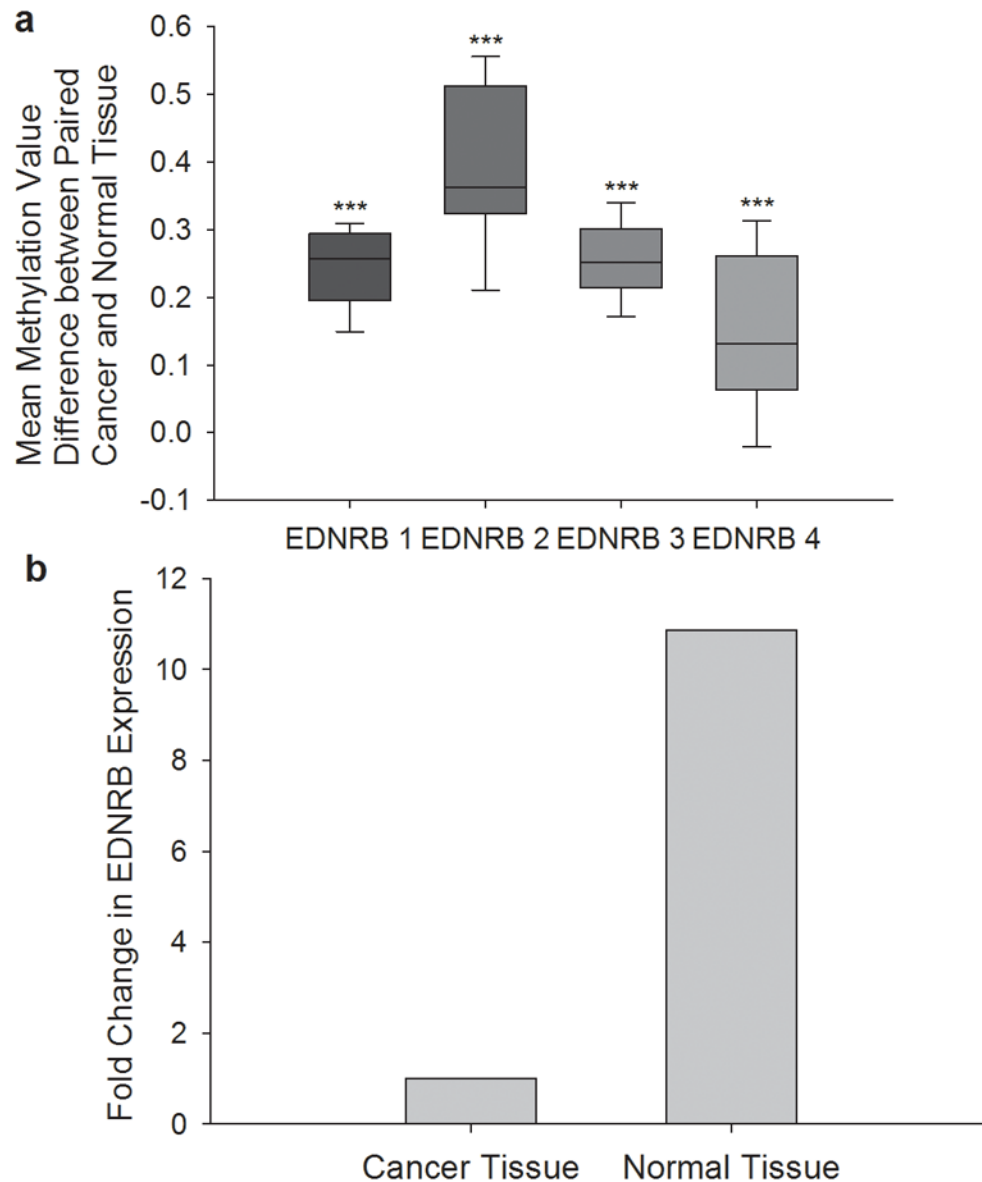


Figure 2.

(a) CpG sites have increased methylation in oral SCC tissue compared to normal tissue

The box plots represent methylation difference values between oral SCC and normal tissue from the same patient. The difference values are averaged from all patients within each CpG site. All CpG sites within a PCR product are grouped together; the median, 10th, 25th, 75th, and 90th percentiles are shown for each group. PCR product EDNRB 2 has the highest increase in methylation in oral SCC tissue (median = 0.34, 34%). EDNRB 1 and 3 have a median increase of 0.25 (25%). EDNRB 4 has the smallest increase of 0.13 (13%).

Methylation values for each sample are averaged across all CpG sites within each PCR product and oral SCC tissue is compared to normal tissue using the Mann Whitney Rank Sum Test (**p<.001). **(b) EDNRB mRNA expression is lower in oral SCC than normal tissue.** EDNRB mRNA expression in normal and oral SCC tissue was quantified using RT-PCR. GUSB was used as the internal locus control. The relative EDNRB mRNA levels was obtained using delta-delta Ct. When compared to oral SCC tissue, normal contralateral

tissue has on average 10.9 times more *EDNRB* mRNA than oral SCC tissue (Student's t test, $p > .001$).

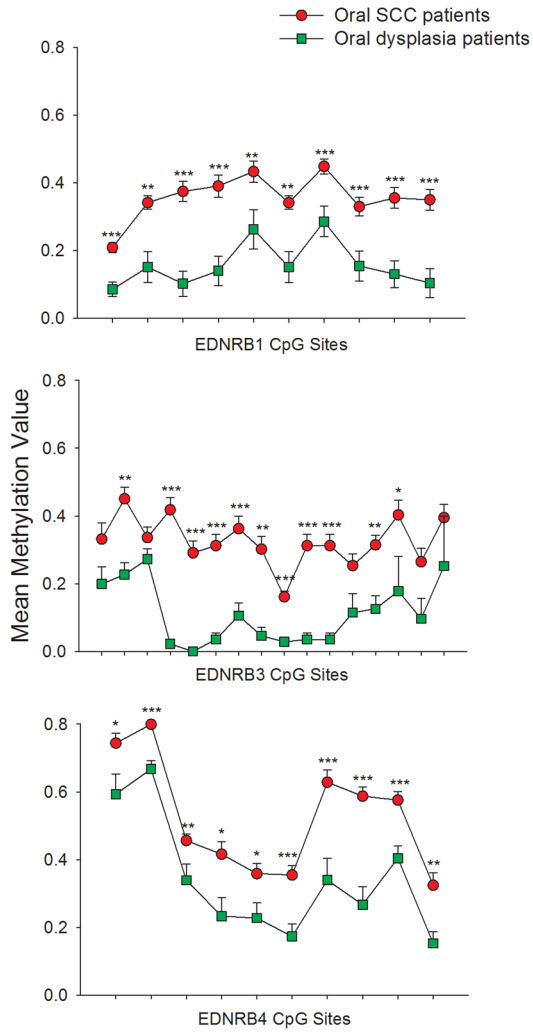


Figure 3. Oral SCC patients demonstrate higher *EDNRB* methylation than oral dysplasia patients

The three plots show methylation values of CpG sites from PCR products EDNRB 1,3, and 4, respectively, in oral SCC and oral dysplasia tissues. Oral SCC tissues exhibit an average of 20% higher methylation than oral dysplasia tissues at all CpG sites. The Mann Whitney Rank Sum Test is used to demonstrate significant differences in methylation between oral SCC and dysplasia tissues (* $p < .05$, ** $p < .01$, *** $p < .001$).

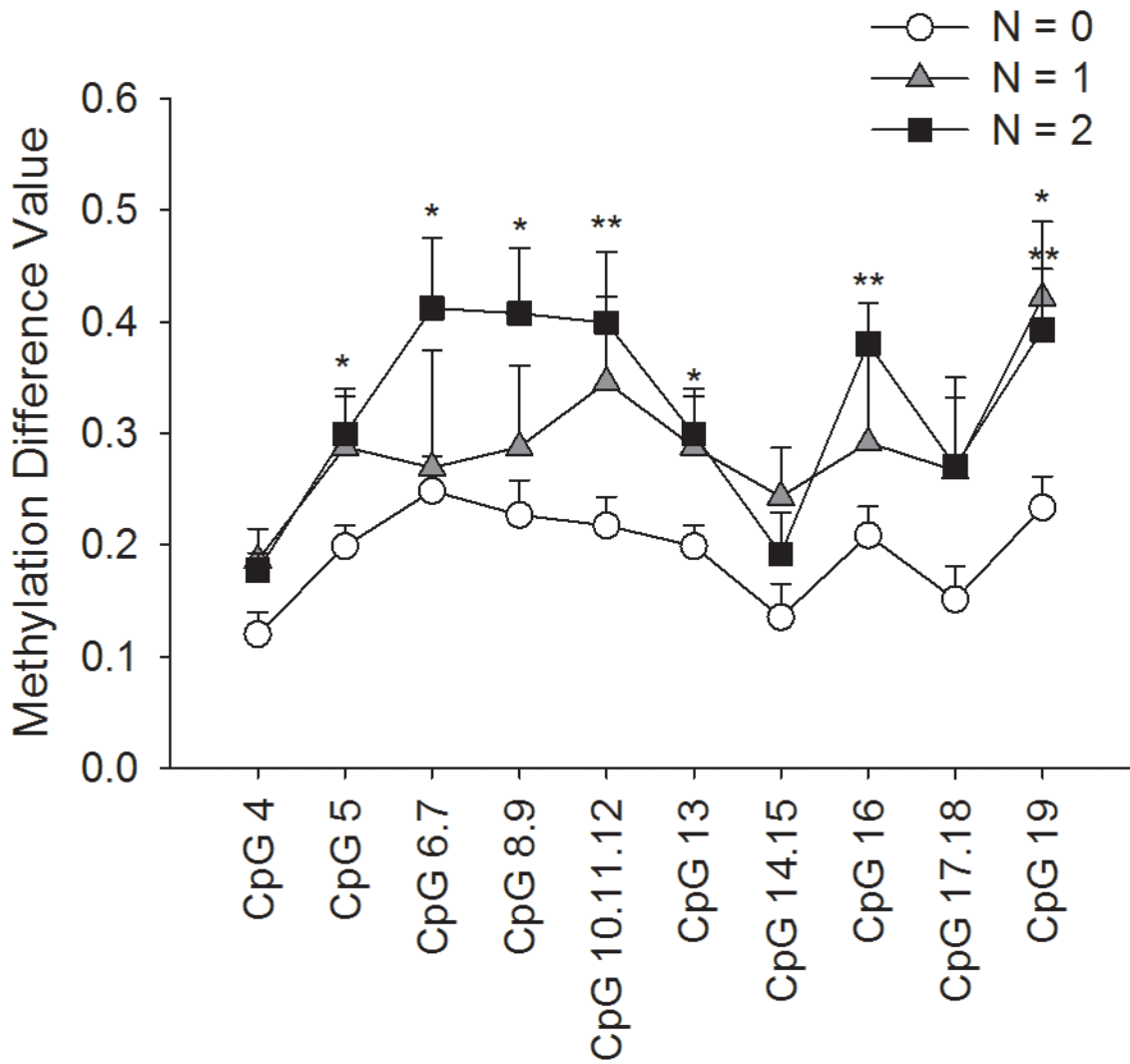


Figure 4. *EDNRB* promoter methylation levels are higher in patients with nodal metastasis
 The graph shows three plots of different nodal metastasis levels. Patients were classified by their TNM staging as N=0, N=1, or N=2. The N=0 group had 11 patients, the N=1 group had 3 patients, and the N=2 group had 6 patients. The plots represent methylation difference values (methylation value of normal tissue subtracted from that of oral SCC tissue) at each CpG unit in the *EDNRB* 1 product, which is the extreme 5' end of the CpG island in the *EDNRB* promoter. The N=0 group has the lowest methylation value differences out of the three groups. The N=1 has intermediate differences, and the N=2 group has the highest methylation value differences. Using ANOVA and the Holm-Sidak test, we showed that the N=2 group is significantly higher than the N=0 group at 7 of 10 CpG units, and that the N=1 group is significantly different from the N=0 group at one CpG unit (*p < .05, **p < .01).

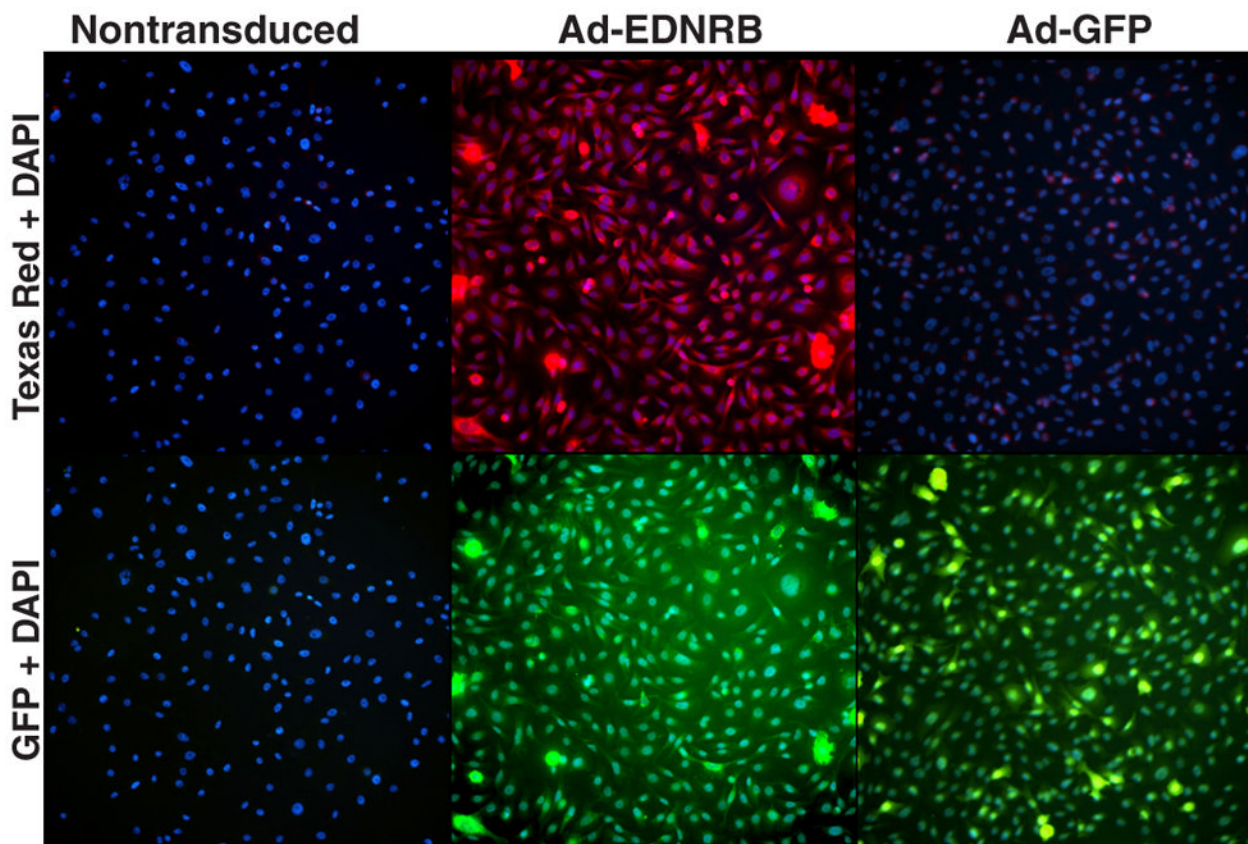


Figure 5. Immunofluorescence images of Ad-EDNRB transduced and nontransduced oral SCC cells

Images are shown at 20X magnification. Images are taken from a single exposure setting. The top row of images shows Texas Red and Hoechst staining. The bottom row of images shows GFP and Hoechst staining. ET_B receptor antibody was secondarily tagged with Texas Red and cell nuclei were counterstained with Hoechst. Nontransduced and Ad-GFP transduced HSC-3 cells display minimal ET_B receptor expression, whereas Ad-EDNRB transduced HSC-3 cells exhibit strong ET_B receptor expression. Ad-GFP transduced HSC-3 cells serve as the positive control for transduction. Ad-GFP transduced HSC-3 cells show strong GFP expression. Ad-EDNRB transduced HSC-3 cells also show GFP expression due to a C-terminal GFP tag on the ET_B receptor protein.

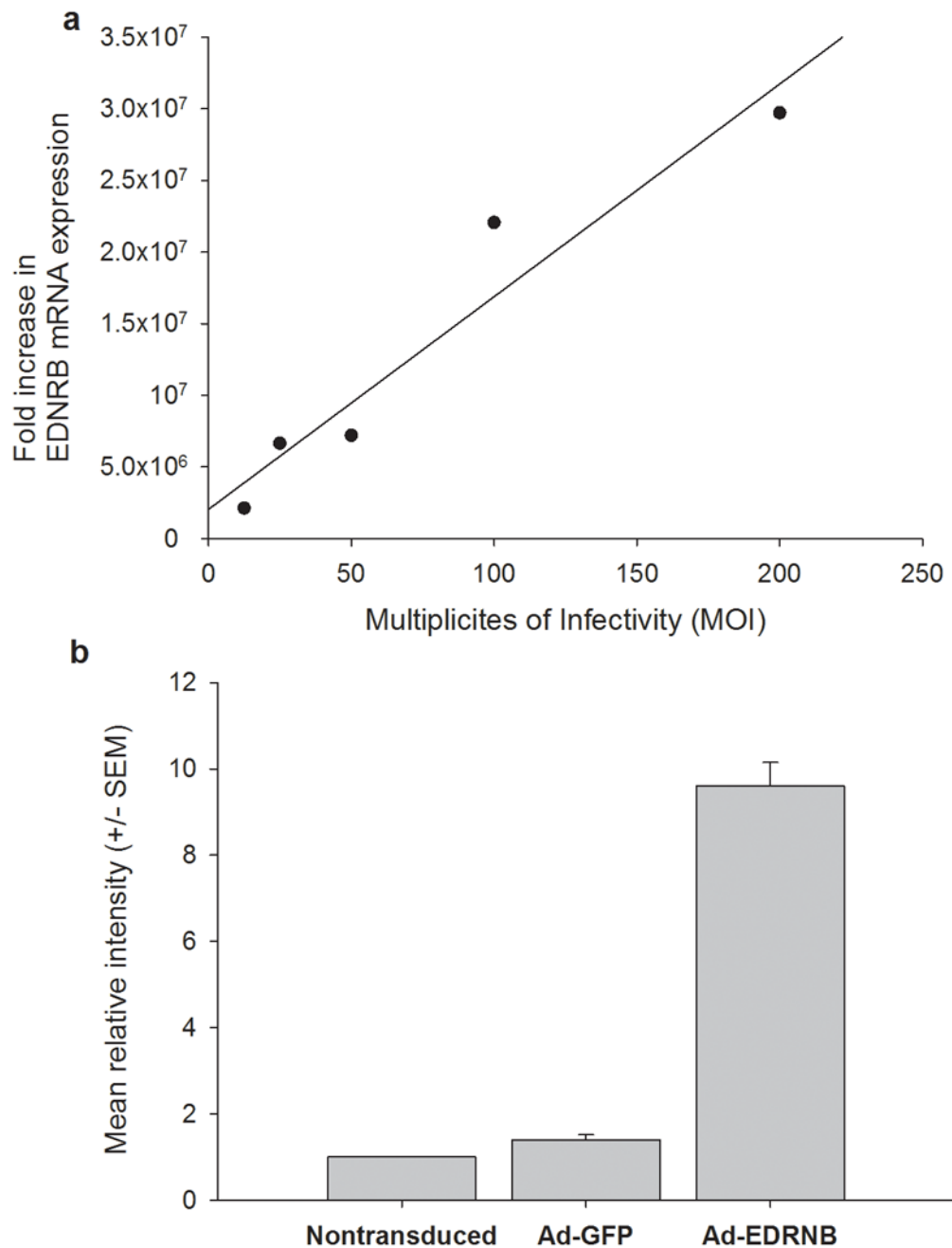


Figure 6.

(a) Oral SCC cells show dose-dependent increase in EDNRB mRNA expression in response to transduction with Ad-EDNRB HSC-3 cells are transduced at 12.5, 25, 50, 100, and 200 MOI. RT-PCR performed on each group reveals that there is a dose-dependent increase in EDNRB mRNA expression with increasing MOI. Fold change is calculated relative to nontransduced HSC-3. **(b) Ad-EDNRB transduced oral SCC cells express high levels of ET_B receptor compared to control oral SCC cells.**

Immunofluorescence images are quantified using Cell Profiler software. ET_B receptor expression is quantified, and relative expression is calculated based on nontransduced HSC-3 expression. Cells transduced with Ad-GFP do not express high levels of ET_B

receptor. However, cells transduced with Ad-EDRN express 9.6 times more ET_B receptor than control, nontransduced cells.

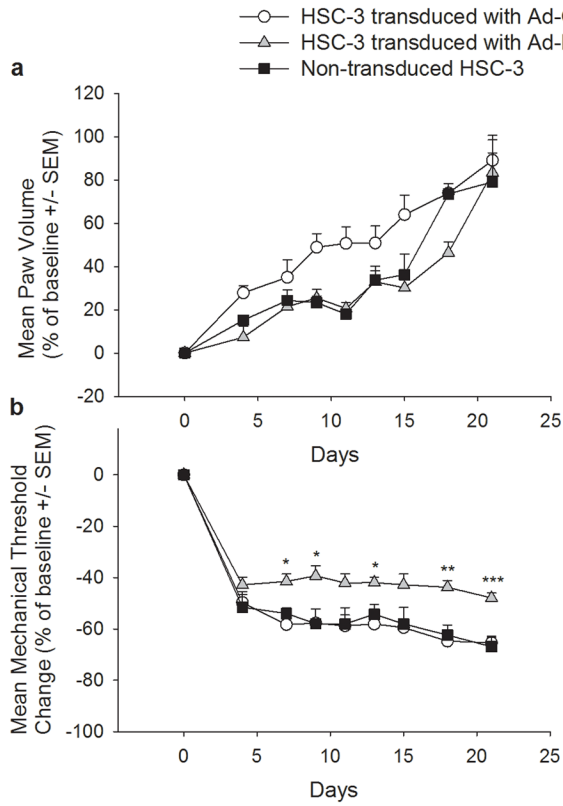


Figure 7.
(a) Ad-EDNRB transduction does not alter oral SCC tumor growth The graph shows change in paw volume, which is a measure of tumor growth. The X axis shows the days of the experiment, and the Y axis shows the average change in paw volume. All three study groups show a similar increase in paw volume as the experiment progresses. There is no statistically significant difference in paw volumes among the study groups. Standard error bars are shown, **(b) Ad-EDNRB transduction decreases mechanical allodynia.** The graph shows change in paw withdrawal threshold, which is a measure of mechanical allodynia. Mice with tumors that have been transduced with Ad-EDNRB exhibit significantly higher paw withdrawal thresholds, indicating lower mechanical allodynia. ANOVA and Holm-Sidak tests are used (*p < .05, **p < .01, ***p < .001). Standard error bars are shown.

Table 1

Patient ID	Sex	Age	Tumor Location	Staging	Differentiation	Staging
ORAL SCC PATIENTS						
1	M	62	mandible	T4aN0Mx	Well	Well
2	F	70	maxilla	T1N0Mx	Well	Well
3	F	62	tongue	T1N0Mx	Moderate	Moderate
4	M	75	tongue	T1N0Mx	Well	Well
5	M	59	buccal mucosa	T2N1Mx	Well	Well
6	M	60	mandible	T1N2bMx	Moderate	Moderate
7	M	49	floor of mouth	T1N2cMx	Moderate	Moderate
8	F	84	mandible	T3N0Mx	Moderate	Moderate
9	M	56	tongue	T1N0Mx	Moderate	Moderate
10	M	51	mandible	T4aN0Mx	Well	Well
11	M	59	mandible	T4aN2bMx	Moderate	Moderate
12	F	84	maxilla	T2N0Mx	Moderate	Moderate
13	F	76	mandible	T3N2bMx	Well-Moderate	Well-Moderate
14	F	59	mandible	T1N1Mx	Poor	Poor
15	F	93	maxilla	T4aN0Mx	Well	Well
16	F	60	mandible	T3N2bMx	Moderate	Moderate
17	F	60	tongue	T2N2bMx	Well	Well
18	M	62	maxilla	T4aN0Mx	Well	Well
19	F	66	tongue	T2N0Mx	Well	Well
20	F	71	tongue	T1N1Mx	Moderate	Moderate
ORAL DYSPLASIA PATIENTS						
1	M	82	floor of mouth	Severe		
2	M	70	tongue	Carcinoma in situ		
3	M	69	tongue	Severe		
4	F	89	maxilla	Mild		
5	M	50	tongue	Carcinoma in situ		
6	M	59	retromolar trigone	Carcinoma in situ		

Patient ID	Sex	Age	Tumor Location	Staging	Differentiation Staging
7	M	51	tongue	Carcinoma in situ	
8	F	75	tongue	Mild	

Table 2

Name	Primer Sequence	5' Position	Amplified Strand
EDNRB-1F	aggagagagagTTATTGATTGAAATTTTATTTTGGGG	-792	Antisense
EDNRB-1R	cagtaatacgcactactataggagagggcTTAAAAACACCTAAAAACCCAAAAAACTT	-425	
EDNRB-2F	aggagagagTAGAGGAAGGAAGATAGGATATTTGG	-63	Sense
EDNRB-2R	cagtaatacgcactactataggagagggcCAAAAACCTTAAACACAAAACCCCTTAACC	-463	
EDNRB-3F	aggagagagTAGTTGAGAGGGTATTAGGAAGGAG	-250	Antisense
EDNRB-3R	cagtaatacgcactactataggagagggcTTAAAAACCCTTAAACCATAAAATCT	176	
EDNRB-4F	aggagagagTGTGTAGTAGGTTTTTTAGAGTTAAAGTTGG	151	Antisense
EDNRB-4R	cagtaatacgcactactataggagagggcAAAAACCTTATAACCCAAAAAATCCA	451	

Table 3

EDNRB PCR Product	CpG Site	Mean Methylation Difference	p-value of Student t test
EDNRB 1	CpG 4	0.15	<.0001
	CpG 5	0.24	<.0001
	CpG 6-7	0.30	<.0001
	CpG 8-9	0.29	<.0001
	CpG 10-11-12	0.29	<.0001
	CpG 13	0.24	<.0001
	CpG 14-15	0.27	<.0001
	CpG 16	0.17	<.0001
	CpG 17-18	0.20	<.0001
	CpG 19	0.30	<.0001
EDNRB 2	CpG 1-2	0.22	<.0001
	CpG 3-4	0.51	<.0001
	CpG 5	0.32	<.0001
	CpG 8	0.34	<.0001
	CpG 9-10	0.19	.0001
	CpG 13-14-15	0.36	<.0001
	CpG 16	0.32	<.0001
	CpG 17	0.51	<.0001
	CpG 18-19	0.55	<.0001
	CpG 20	0.36	<.0001
	CpG 21	0.56	<.0001
	CpG 22-23	0.43	<.0001
	CpG 24	0.36	<.0001
	CpG 25	0.39	<.0001
CpG 26	0.39	<.0001	
EDNRB 3	CpG 1	0.23	.0001
	CpG 2-3-4	0.27	<.0001
	CpG 5	0.21	<.0001
	CpG 6-7	0.37	<.0001
	CpG 8	0.32	<.0001
	CpG 9	0.26	<.0001
	CpG 10-11	0.33	<.0001
	CpG 12	0.28	<.0001
	CpG 14	0.14	.0002
	CpG 15	0.26	<.0001
	CpG 16	0.26	<.0001
	CpG 18	0.19	<.0001
CpG 19	0.22	<.0001	

EDNRB PCR Product	CpG Site	Mean Methylation Difference	p-value of Student t test
	CpG 20	0.32	<.0001
	CpG 27	0.19	<.0001
	CpG 28	0.31	<.0001
EDNRB 4	CpG 1	-0.03	.4728
	CpG 2-3	0.02	.3934
	CpG 4	0.10	.0557
	CpG 6	0.16	.0011
	CpG 7	0.08	.0084
	CpG 8	0.10	.0082
	CpG 9-10	0.27	<.0001
	CpG 12	0.32	<.0001
	CpG 14-15	0.26	<.0001
	CpG 16	0.20	.0003